Effect of Asp-235 → Asn Substitution on the Absorption Spectrum and Hydrogen Peroxide Reactivity of Cytochrome *c* Peroxidase†

Lidia B. Vitello,‡ James E. Erman,*,‡ Mark A. Miller,§ J. Matthew Mauro,§,∥ and Joseph Kraut§

Department of Chemistry, Northern Illinois University, DeKalb, Illinois 60115, and Department of Chemistry, University of California, San Diego, La Jolla, California 92093

Received April 24, 1992; Revised Manuscript Received September 4, 1992

ABSTRACT: The spectroscopic properties of a mutant cytochrome *c* peroxidase, in which Asp-235 has been replaced by an asparagine residue, were examined in both nitrate and phosphate buffers between pH 4 and 10.5. The spin state of the enzyme is pH dependent, and four distinct spectroscopic species are observed in each buffer system: a predominantly high-spin Fe(III) species at pH 4, two distinct low-spin forms between pH 5 and 9, and the denatured enzyme above pH 9.3. The spectrum of the mutant enzyme at pH 4 is dependent upon specific ion effects. Increasing the pH above 5 converts the mutant enzyme to a predominantly low-spin hydroxy complex. Subsequent conversion to a second low-spin form is essentially complete at pH 7.5. The second low-spin form has the distal histidine, His-52, coordinated to the heme iron. To evaluate the effect of the changes in coordination state upon the reactivity of the enzyme, the reaction between hydrogen peroxide and the mutant enzyme was also examined as a function of pH. The reaction of CcP(MI,D235N) with peroxide is biphasic. At pH 6, the rapid phase of the reaction can be attributed to the bimolecular reaction between hydrogen peroxide and the hydroxy-ligated form of the mutant enzyme. Despite the hexacoordination of the heme iron in this form, the bimolecular rate constant is ~22% that of pentacoordinate wild-type yeast cytochrome *c* peroxidase. The bimolecular reaction of the mutant enzyme with peroxide exhibits the same pH dependence in nitrate-containing buffers that has been described for the wild-type enzyme, indicating a loss of reactivity with the protonation of a group with an apparent pK_a of 5.4. This observation eliminates Asp-235 as the source for this heme-linked ionization and strengthens the hypothesis that the pK_a of 5.4 is associated with His-52. The slower phase of the reaction between peroxide and the mutant enzyme saturates at high peroxide concentration and is attributed to conversion of unreactive to reactive forms of the enzyme. The fraction of enzyme which reacts via the slow phase is dependent upon both pH and specific ion effects.

Comparisons of the three-dimensional structures of myoglobin and yeast cytochrome *c* peroxidase (ferrocytochrome *c*:H_2O_2 oxidoreductase, EC 1.11.1.5) have been useful in developing ideas about structure/function relationships in heme proteins (Poulos et al., 1980; Poulos & Finzel, 1984). The heme pocket of CcP[1] is more polar than that of myoglobin and favors stabilization of the Fe(III) heme relative to that of myoglobin. In particular, there are two charged groups in the heme pocket of CcP, Arg-48 and Asp-235, which have no counterpart in myoglobin but are present in other peroxidases (Poulos & Finzel, 1984). It has been suggested that Arg-48, a distal-side residue, plays a role in the reaction between CcP and hydrogen peroxide by stabilizing the transition state of the peroxide cleavage reaction (Poulos & Kraut, 1980). Asp-235 hydrogen bonds to the proximal heme ligand, His-175. Three distinct roles have been suggested for this interaction: first, to maintain the open sixth coordination site, allowing the very fast reaction with peroxide; second, to accelerate the heterolytic cleavage of peroxide by increasing the donation of electron density from the iron toward the π orbitals of the coordinated ligand; and third, to stabilize the oxyferryl state by adding electron density to the heme iron (Wang et al., 1990; Smulevich et al., 1991). In order to explore the functional role of Asp-235, we have investigated the properties of a mutant CcP expressed in *Escherichia coli* (Fishel et al., 1987) in which Asp-235 has been replaced by asparagine, CcP(MI,D235N). In this report we compare the properties of CcP(MI,D235N) with those of CcP(MI), the parent CcP expressed in *E. coli*, and those of wild-type CcP isolated from yeast.

We have confirmed the previously made conclusions (Smulevich et al., 1988) that the Asp-235 → Asn mutation dramatically alters the ligation at the sixth coordination site of the heme iron. Our results show that, while the Asp-235 to His-175 interaction is required to maintain pentacoordination of the heme iron in the neutral pH region, hexacoordination in the mutant enzyme only decreases the hydrogen peroxide reaction rate by a factor of 4–5. Moreover, the oxyferryl state is quite stable in this mutant, suggesting that Asp-235 is not necessary to stabilize the higher oxidation states of the enzyme.

Many of the kinetic and spectroscopic properties of CcP are pH dependent in buffers containing nitrate as supporting electrolyte. A heme-linked ionization with an apparent pK_a of about ~5.4 in 0.1 M ionic strength buffers influences the reaction with hydrogen peroxide (Loo & Erman, 1975) and

† This work was supported in part by Research Grants NSF DMB 87-16459 and PHS 1R15 DK43944 to J.E.E. and L.B.V., NSF DMB 88-15718 to J.K., NRSA Postdoctoral Fellowship PHS GM 10292 to J.M.M., and a postdoctoral fellowship from Hemoglobin and Blood Training Grant 5 T32 AM07233-11 to M.A.M.

* Author to whom correspondence should be addressed.

‡ Northern Illinois University.

§ University of California, San Diego.

∥ Present address: Center for Advanced Research in Biotechnology, 9600 Gudelsky Drive, Rockville, MD 20850.

[1] Abbreviations: CcP, cytochrome *c* peroxidase; CcP(MI), recombinant cytochrome *c* peroxidase expressed in *E. coli*; CcP(MI,D235N), the Asp-235 → Asn mutant of CcP(MI); hs, high-spin form of CcP(MI,D235N) observed at low pH; ls1, low-spin form of the mutant enzyme with hydroxy-ligated heme; ls2, second low-spin form of the mutant enzyme with the distal histidine coordinated to the heme iron.

0006-2960/92/0431-11524$03.00/0

binding of fluoride (Lent et al., 1976) and cyanide (Erman, 1974) and causes small perturbations in the electronic absorption spectrum (Conroy & Erman, 1978; Vitello et al., 1990b) and in the resonance Raman spectrum (Shelnutt et al., 1983). The ionization of Asp-235 has been suggested as a possible cause for these pH-dependent properties of yeast CcP (Poulos & Finzel, 1984; Edwards et al., 1984). In this report we show that the CcP(MI,D235N)/hydrogen peroxide reaction depends upon an enzyme ionization with an apparent pK_a of 5.4 in nitrate-containing buffers just as in the wild-type yeast CcP. This observation eliminates Asp-235 as the source for this heme-linked ionization.

MATERIALS AND METHODS

Twice-crystallized CCP(MI,D235N) was prepared as previously described (Fishel et al., 1987). Concentrations of the enzyme were determined spectroscopically in 0.1 M phosphate buffer, pH 6, using a millimolar absorptivity of 110 at 413 nm (Smulevich et al., 1988). Hydrogen peroxide (30%, J. T. Baker Chemical Co.) was standardized with cerium(IV) sulfate according to Kolthoff & Belcher, 1957.

Two buffer systems were used in this study. The first series were 10 mM in buffering components with added KNO_3 to adjust the ionic strength to 0.1 M; acetate, phosphate, tris, and glycine were used as the buffering components in the appropriate pH regions. The second series of buffers were 0.1 M in total phosphate concentration. These latter buffers were made by mixing appropriate amounts of 0.1 M H_3PO_4, 0.1 M KH_2PO_4, and 0.1 M K_2HPO_4 while the pH was monitored. The 0.1 M phosphate buffers have low buffering capacity below pH 6, and although their ionic strength is essentially constant between pH 4 and 6, the ionic strength of these buffers increases substantially between pH 6 and 8. The phosphate buffers were used to compare properties of CcP(MI,D235N) with those of CcP(MI) and wild-type yeast CcP under identical experimental conditions since the reaction between CcP and hydrogen peroxide is significantly different in phosphate and in nitrate-containing buffers (Balny et al., 1987; Vitello et al., 1990b).

To investigate the pH-dependent properties of CcP(MI,D235N), stock solutions of the enzyme were made in unbuffered 0.1 M KNO_3 (pH ~5.3) or 0.1 M KH_2PO_4 (pH ~4.5), depending upon the buffer system to be used. Small aliquots (less than 5% of the final volume) of stock enzyme were added to the desired buffer and the experiments performed. For those buffers which have low buffering capacity, the pH of the solution was measured before and after each experiment. Spectral properties of the enzyme were determined immediately after mixing the enzyme into each buffer solution. Spectra were obtained at a scan rate of 1 nm/s with a Cary Model 219 spectrophotometer.

The stoichiometry of the reaction between hydrogen peroxide and the enzyme was determined as a function of pH. The titrations were usually carried out by adding multiple aliquots of standardized hydrogen peroxide to an enzyme sample, monitoring the change in absorbance at 427 nm upon each peroxide addition, and continuing until a maximum change in absorbance was detected.

The rates of the hydrogen peroxide/enzyme reaction were studied using either a Durrum-Gibson stopped-flow spectrophotometer, Model D-110 (Dionex Corp.), or a HI-Tech Scientific Model PQ/SF-53 stopped-flow instrument. Reactant syringes, mixer, and observation chamber were maintained at 25 ± 1 °C with a circulating water bath. The reactions were studied under pseudo-first-order conditions with hydrogen peroxide in excess. Enzyme concentrations ranged from 0.2 to 1.0 μM and hydrogen peroxide from 2 to 40 μM.

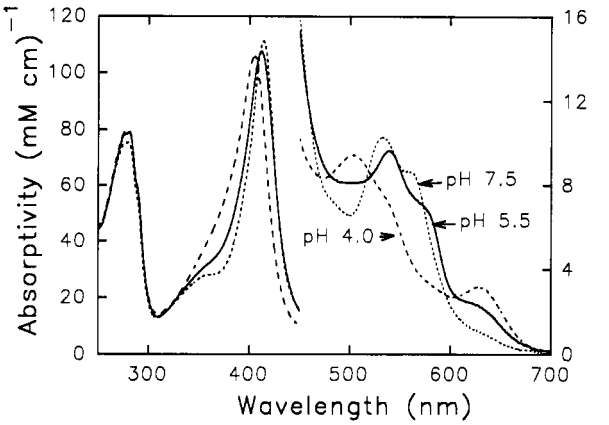

FIGURE 1: Spectrum of CcP(MI,D235N) in nitrate-containing buffers.

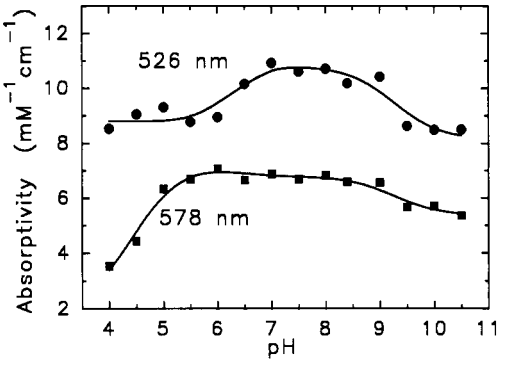

FIGURE 2: Variation of the absorptivity of CcP(MI,D235N) at two wavelengths in nitrate-containing buffers. The apparent pK_a's for the transitions are 4.4 ± 0.3, 6.3 ± 0.4, and 9.3 ± 0.4. The solid lines were calculated from the model shown in Figure 8.

RESULTS

pH Dependence of the Electronic Absorption Spectrum in Buffers Containing Nitrate. The electronic absorption spectrum of the mutant enzyme, CcP(MI,D235N), is significantly different from that of parental CcP(MI) or of wild-type yeast CcP at neutral pH. In addition, the absorption spectrum of CcP(MI,D235N) varies significantly between pH 4 and pH 7.5, a pH region where the spectra of CcP(MI) and native yeast CcP change very little. Figure 1 shows the spectrum of CcP(MI,D235N) at pH 4.0, 5.5, and 7.5 in buffers which contain KNO_3 to adjust the ionic strength to 0.1 M. The three spectra do not have isosbestic points, indicating that more than two spectroscopic forms of the enzyme exist within this pH range. The pH dependence of the spectrum is most readily observed in the visible region. Figure 2 presents plots of the absorptivity at 526 and 578 nm as a function of pH. Spectra were acquired at each half pH unit between pH 4 and 10.5, a pH at which the enzyme has undergone alkaline denaturation. Three transitions are readily apparent. The absorptivity at 526 nm is relatively constant between pH 4 and pH 6, increases between pH 6 and 7, and decreases again above pH 8.5. On the other hand, the absorptivity at 578 nm increases significantly between pH 4 and 6, remains relatively constant between pH 6 and 8.5, and decreases above pH 8.5. The pH dependence of the spectra can be expressed in terms of four spectroscopically distinct species, interrelated by three apparent pK_a values according to eq 1. The pK_a's are numbered to correspond to a model presented later. In anticipation of

$$H_3E(hs) \underset{pK_1}{\rightleftharpoons} H_2E(ls1) \underset{pK_5}{\rightleftharpoons} HE(ls2) \underset{pK_7}{\rightleftharpoons} E(d) \quad (1)$$

our conclusions, we represent the spectroscopically distinct mutant enzyme species to indicate the predominant spin state of each species. The enzyme species which predominates at pH 4 is represented as H_3E(hs). It is a high-spin form of the mutant enzyme. Deprotonation of H_3E(hs) produces H_2E(ls1), a hexacoordinate, low-spin form of CcP(MI,D235N). The second transition, characterized by pK_5, produces a second, distinct, hexacoordinate, low-spin form of the mutant enzyme, HE(ls2). The third transition, characterized by pK_7, produces denatured enzyme, E(d). Nonlinear, least-squares regression analysis of the pH dependence of the absorptivities at multiple wavelengths was used to determine the apparent pK_a values, and they are collected in Table I.

The spectra shown in Figure 1 are those of various mixtures of the enzyme forms defined in eq 1, although one particular form dominates at each pH. Spectra of the individual species can be calculated from the pH dependence of the observed spectra and the apparent pK_a values. The relevant spectroscopic parameters for the three nondenatured forms of CcP(MI,D235N) defined in eq 1 are collected in Table II.

Hydrogen Peroxide Titer in Buffers Containing Nitrate. CcP(MI,D235N) reacts with hydrogen peroxide to form a spectroscopically distinct species (Figure 3). The maximum difference occurs at 427 nm, and this spectroscopic change can be used to determine the stoichiometry of the hydrogen peroxide/mutant enzyme reaction. The stoichiometry was determined as a function of pH between pH 4 and 9 in KNO_3-containing buffers, and the results are shown in Figure 4A along with the data for CcP(MI). The maximum stoichiometric ratio for the mutant enzyme occurs at pH 5.5, where 85% of the enzyme reacts with hydrogen peroxide. The stoichiometric ratio decreases to 20% at pH 4.0, the lowest pH investigated, and no detectable compound I formation from the mutant enzyme was observed at pH 8.0 and above (Figure 4A). The pH dependence of the peroxide/enzyme stoichiometry indicates that conversion of the enzyme to acidic or alkaline forms inactivates the enzyme in its reaction with hydrogen peroxide.

Even though the loss of peroxide titer at acidic pH coincides with the conversion of the ls1 to hs forms of the enzyme, additional evidence indicates that the enzyme which reacts with peroxide at pH 4 is, in fact the hs form. We have calculated the change in absorptivity upon reaction with hydrogen peroxide, ΔE_{427}, by dividing the observed absorbance change by the concentration of reactive enzyme. The ΔE_{427} values vary between 52 ± 3 and 26 ± 2 mM^{-1} cm^{-1} between pH 4 and pH 7, respectively (Figure 4B). This variation is consistent with a predominantly high-spin form of CcP(MI,D235N) being converted to I at pH 4 and a low-spin form of the enzyme being oxidized to I at pH 7. Also shown in Figure 4B is the difference in absorptivity at 424 nm (the wavelength of maximum difference) for the conversion of CcP(MI) to I. The absorptivity difference is 44 ± 2 mM^{-1} cm^{-1}, independent of pH, for the CcP(MI)/hydrogen peroxide reaction. CcP(MI) is a pentacoordinate, high-spin Fe(III) protein between pH 4.5 and 7 (Smulevich et al., 1988; Vitello et al., 1990a). The value of ΔE_{427} at pH 4 for conversion of the reactive form of CcP(MI,D235) to I is larger than that for CcP(MI) because of the blue-shifted Soret band for the high-spin form of the Asn mutant compared to the Soret band of CcP(MI) (Table II). The decrease in ΔE_{427} for the reactive form of the Asn mutant with increasing pH is due to the conversion of CcP(MI,D235N) to a low-spin form and the associated red shift of the Soret band (Table II), decreasing the difference in absorbance between the Fe(III) and Fe(IV) states of the enzyme.

Table I: pK_a Values Defined in Figure 8 and Used To Fit the pH Dependence of the Experimental Data

pK_a	nitrate[a]	phosphate[b]	property[c]
pK_1	4.4 ± 0.3	5.0 ± 0.2	hs ⇌ ls1 spectral transition
pK_2	4.4 ± 0.2	5.5 ± 0.6	transition to low-pH, inactive hs and ls1 species
pK_3	5.4 ● 0.1	4.7 ± 0.1	pH dependence of k_1
pK_4	6.0 ± 0.1	7.7 ± 0.6	transition to high-pH, inactive form of ls1
pK_5	6.3 ± 0.4	6.6 ± 0.4	ls1 ⇌ ls2 spectral transition
pK_6	7.0 ± 0.1[d]	7.5 ± 0.3	transition to high-pH, inactive form of ls2
pK_7	9.3 ± 0.4		transition between ls2 and denatured enzyme

[a] Buffers using KNO_3 to adjust ionic strength to 0.1 M. [b] Phosphate buffer, 0.1 M. [c] Experimental property affected by apparent pK_a. [d] Requires cooperative, two-proton dissociation to fit the experimental data.

The experimental spectrum for the peroxide-oxidized form, of CcP(MI,D235N) (Figure 3) does not represent the spectrum of compound I since only 75 ± 4% of the enzyme reacts with hydrogen peroxide at this pH. In the Discussion section we will present a model which accounts for the pH-dependent properties of CcP(MI,D235N). This model indicates that the spectrum of the peroxide-oxidized product at pH 6 is 75% I and 25% of the unconverted ls1 form of the mutant enzyme. We can calculate the spectrum of I by subtracting the contribution of the unreacted ls1 form of the enzyme and normalizing the resulting spectrum for 100% conversion to I. The calculated spectrum of CcP(MI,D235N) I is shown in Figure 3, and its spectroscopic parameters are collected in Table II. The spectroscopic parameters are very similar to those of CcP(MI) compound I.

Hydrogen Peroxide/CcP(MI,D235N) Kinetics in Buffers Containing Nitrate. The kinetics of the reaction between CcP(MI,D235N) and hydrogen peroxide are complex. In general, two reaction phases are evident. The reactions can be characterized by two first-order rate constants designated k_A and k_B. The fast phase of the reaction, rate constant k_A, is observed between pH 4.0 and 6.5 with a maximum amplitude occurring at pH 5 (Figure 5). k_A is linearly dependent upon the hydrogen peroxide concentration between 2 and 40 μM under all conditions investigated. Apparent bimolecular rate constants, k_1^{app}, are obtained from the slope of plots of k_A versus hydrogen peroxide. Values of k_1^{app} varied between 1.1 ± 0.3 × 10^5 M^{-1} s^{-1} at pH 4.5 and 8.5 ± 1.5 × 10^6 M^{-1} s^{-1} at pH 6.5. A plot of log k_1^{app} versus pH is shown in Figure 6. The apparent bimolecular rate constant is dependent upon pH in nitrate-containing buffers, as has been observed for yeast CcP (Loo & Erman, 1975; Vitello et al., 1990b). The enzyme is active when a critical residue in the enzyme is deprotonated and inactive when the enzyme is protonated. If the protonated and deprotonated states of the residue equilibrate rapidly compared to the rate of the hydrogen peroxide reaction, the pH dependence of the apparent rate constant is given by eq 2, where K_3 is the acid dissociation constant for

$$k_1^{app} = k_1 K_3/(K_3 + [H^+]) \quad (2)$$

the critical residue. Fitting the apparent bimolecular rate constant to eq 2 gives best-fit values of 11 ± 5 μM^{-1} s^{-1} for the pH-independent rate constant and a pK_3 value of 5.4 ± 0.1 for the reaction between the active conformer of

Table II: Spectroscopic Parameters for the Various pH-Dependent Forms of CcP(MI,D235N) and CcP(MI)

protein[a]	species[b]	buffer	visible region absorption bands[c]				
			Soret	CT1	β	α	CT2
MI	hs	nitrate	408 (102)	508 (11.5)	540 (9.3, sh)	592 (2.3, sh)	644 (3.4)
MI,D235N	hs	nitrate	403 (110)	504 (9.9)	539 (6.1, sh)	595 (2.3, sh)	630 (3.5)
MI,D235N	hs	phosphate	406 (135)	500 (8.4)	535 (5.5, sh)	576 (4.3)	624 (6.4)
MI,D235N	ls1	nitrate	412 (109)	501 (8.2, sh)	541 (9.9)	576 (7.5, sh)	627 (2.3, sh)
MI,D235N	ls1	phosphate	412 (109)	503 (8.1, sh)	541 (9.9)	576 (7.7)	627 (1.7, sh)
MI	ls	nitrate	414 (102)	488 (8.6, sh)	534 (10.4)	563 (8.3, sh)	629 (2.9, sh)
MI,D235N	ls2	nitrate	414 (112)	486 (6.8, sh)	532 (10.4)	566 (8.4, sh)	632 (0.9, sh)
MI,D235N	ls2	phosphate	414 (113)	485 (7.7, sh)	531 (10.9)	566 (8.8, sh)	634 (1.3, sh)
MI	I	nitrate	419 (106)		530 (12.2)	560 (13.1)	627 (4.5, sh)
MI,D235N	I	nitrate	419 (101)		529 (12.5)	559 (13.7)	631 (2.4, sh)

[a] CcP(MI) and CcP(MI,D235N) are identified as MI and MI,D235N, respectively. [b] The various Fe(III) heme species are identified as hs (high-spin), ls (low-spin), and, for the two CcP(MI,D235N) low-spin species, ls1 and ls2. Compound I spectral parameters are also included. [c] Wavelength maximum given in nanometers, followed by the millimolar absorptivity in parenthesis. Shoulders or inflections in the spectra are identified by an "sh".

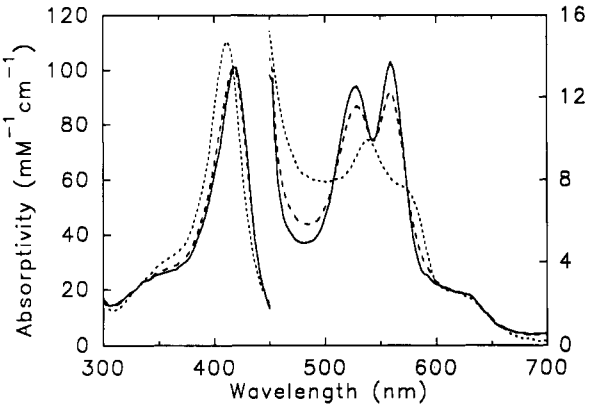

FIGURE 3: Spectrum of CcP(MI,D235N) and CcP(MI,D235N) compound I at pH 6.0 in nitrate-containing buffers: short dashed line, CcP(MI,D235N); medium dashed line, observed hydrogen peroxide product; solid line, CcP(MI,D235N) compound I spectrum calculated for 100% conversion of the enzyme. Under these experimental conditions, hydrogen peroxide only converts 75% of CcP(MI,D235N) to I. The fraction of CcP(MI,D235N converted to I and the spectrum of I are independent of the two buffer systems used at pH 6.

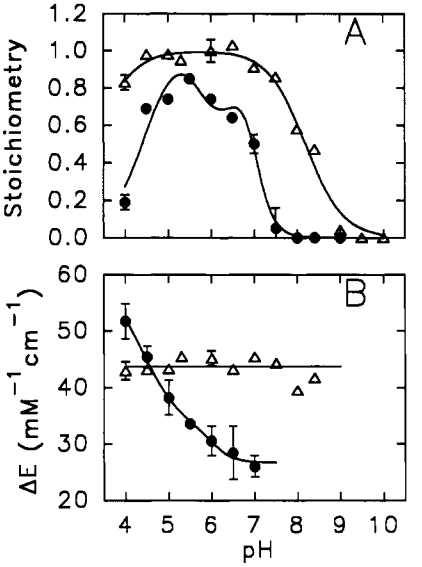

FIGURE 4: (A) Hydrogen peroxide titer of CcP(MI,D235N) as a function of pH in nitrate-containing buffers: solid circles, CcP(MI,D235N); open triangles, CcP(MI), data from Vitello et al. (1990a). The solid line for the CcP(MI,D235N) data was calculated from the model shown in Figure 8. (B) Change in absorptivity for the conversion of reactive enzyme to I: solid circles, CcP(MI,D235N) at 427 nm; open triangles, CcP(MI) at 424 nm.

CcP(MI,D235N) and hydrogen peroxide. The value of k_1 is ~24% of the value for CcP(MI) and wild-type yeast CcP, which have pH-independent rate constants of 47 ± 5 and 45 ± 6 μM^{-1} s^{-1}, respectively (Vitello et al., 1990a). The value of pK_3 is identical for CcP(MI,D235N), CcP(MI), and wild-type CcP; all three enzymes give best-fit values of 5.4 for the value of pK_3 (Vitello et al., 1990a).

The slow phase of the reaction is only observed between pH 5 and 7. The amplitude of this phase of the reaction is generally much smaller than that of the fast phase (Figure 5), although at pH 7, only the slow phase is observed. The small amplitude of the slow reaction makes it difficult to obtain accurate data, but k_B appears to be independent of the hydrogen peroxide concentration between 2 and 40 μM. Our interpretation is that k_B represents the isomerization of the enzyme from an inactive conformation to an active form which reacts rapidly with hydrogen peroxide. In Figure 6, we report the average values of k_B, which vary between 0.15 and 1.7 s^{-1} as a function of pH. The values of k_B are designated k_B^{max} in Figure 6 since these values appear to be saturation values (see below). The average standard deviation for k_B is 46%.

Effect of Specific Ions on the Absorption Spectrum of CcP(MI,D235N). The kinetics of the reaction between hydrogen peroxide and yeast CcP are significantly different in phosphate and nitrate-containing buffers (Vitello et al., 1990b), and in this study of the Asn-235 mutant we have used both types of buffers. In addition to differences in the kinetic properties (see below), the absorption properties of CcP(MI,D235N) also depend upon the nature of the buffer. Above pH 6, the absorption spectrum of CcP(MI,D235N) is essentially identical in the two buffer systems used in this study. However the spectrum at pH 4 is quite different (Figure 7). There is a 3-nm red shift and a 20% increase in the absorptivity at the Soret maximum in phosphate buffer in comparison to the enzyme in nitrate-containing buffers. In addition the long-wavelength charge-transfer band shifts from 630 nm in nitrate-containing buffers to 624 nm in phosphate buffers along with an 85% increase in absorptivity.

Just as in nitrate-containing buffers, the pH dependence of the spectrum in phosphate buffers indicates that there are more than two spectroscopically distinct species between pH 4 and 8. Two transitions are observed between pH 4 and 8, with values of 5.0 ± 0.2 and 6.6 ± 0.4 for pK_1 and pK_5, respectively (Table I). pK_1 depends upon the nature of the buffer, with values of 4.4 ± 0.2 and 5.0 ± 0.2 in nitrate and phosphate buffers, respectively. pK_5 is independent of buffer composition, within our experimental error. The fraction of the various enzyme forms at each pH can be calculated from

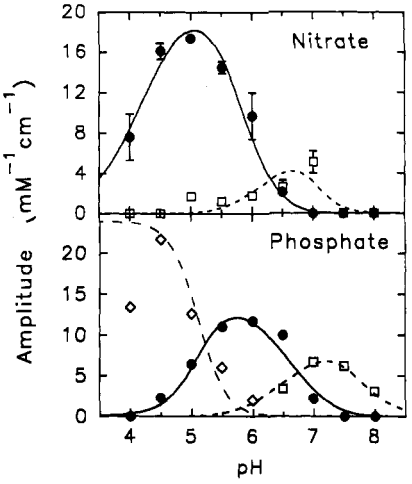

FIGURE 5: (Top panel) pH dependence of the reaction amplitude of the two kinetic phases in nitrate-containing buffer: solid circles, amplitude of the fast phase, characterized by k_A; open squares, amplitude of the slow phase, characterized by k_B. The lines were calculated from the model shown in Figure 8. (Bottom panel) Amplitude of the two kinetic phases for the reaction between CcP(MI,D235N) and hydrogen peroxide in phosphate buffers: solid circles, the fast, bimolecular phase; open squares, amplitude of k_B at high pH; open diamonds, amplitude of k_B at low pH. The lines were calculated from the model shown in Figure 8.

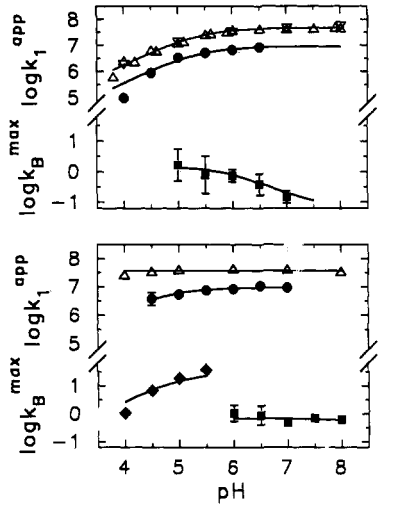

FIGURE 6: (Top panel) pH dependence of the kinetic parameters for the enzyme/hydrogen peroxide reaction in nitrate-containing buffers. Apparent bimolecular rate constant: solid circles, CcP(MI,D235N); open inverted triangles, CcP(MI), data from Vitello et al. (1990a); open triangles, yeast CcP, data from Loo and Erman (1975); solid squares, average value of the slow, hydrogen peroxide-independent rate constant designated k_B^{max}. The lines are calculated according to the model shown in Figure 8. (Bottom panel) pH dependence of the kinetic parameters for the CcP(MI,D235N)/hydrogen peroxide reaction in phosphate buffers: open triangles, apparent bimolecular rate constant for yeast CcP, data from Vitello et al. (1990a); solid circles, apparent bimolecular rate constant for CcP(MI,D235N); solid squares, average value of k_B between pH 6 and 8; solid diamonds, k_B^{max} values calculated from eq 3 between pH 4 and 5.5. The lines were calculated from the model shown in Figure 8.

the experimentally determined pK_a values. The spectroscopic parameters for the individual species in phosphate buffers can then be determined (Table II).

Hydrogen Peroxide/CcP(MI,D235N) Kinetics in Phosphate Buffers. The kinetics of the reaction between CcP(MI,D235N) and hydrogen peroxide are biphasic between pH 4.5 and 7 in phosphate buffers. Just as in nitrate-containing buffers, the reactions can be characterized by two first-order rate constants, k_A and k_B. However, both the amplitudes of

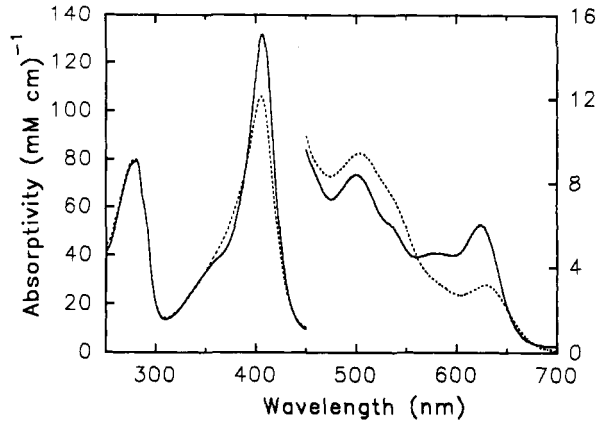

FIGURE 7: Spectrum of CcP(MI,D235N) at pH 4.0: solid line, in phosphate buffer; dashed line, in nitrate-containing buffer.

the two kinetic phases and the pH dependence of the rate constants depend upon the nature of the buffer.

Under pseudo-first-order conditions, with hydrogen peroxide in excess, k_A is linearly dependent on the hydrogen peroxide concentration just as in nitrate-containing buffers, and apparent bimolecular rate constants can be determined. The fast phase of the reaction is only observed between pH 4.5 and 7.0 and has a maximal amplitude at pH 6.0 (Figure 5). The apparent bimolecular rate constant is pH dependent in phosphate buffers (Figure 6). Fitting the data acquired in phosphate buffer to eq 2 gives a value of 9.4 ± 0.8 μM^{-1} s^{-1} for the pH-independent rate constant, k_1, and 4.7 ± 0.1 μM^{-1} s^{-1} for the apparent pK_3 value. The values of k_1 are within experimental error for the two buffer systems, while pK_3 is significantly different.

In buffers using nitrate as supporting electrolyte, the amplitude of the slow phase is quite small and is observed only above pH 5, reaching maximum amplitude near pH 7 (Figure 5). In phosphate buffers, the slow phase of the reaction is observed over the entire pH region investigated, pH 4–8, and becomes the dominant phase below pH 5 (Figure 5). The amplitude of the slow phase of the CcP(MI,D235N)/hydrogen peroxide reaction in phosphate buffer has two local maxima, one near pH 4.5 and the other near pH 7. We believe that there are two distinct slow reactions in phosphate buffers, one between hydrogen peroxide and an acidic conformer of the mutant enzyme and one with a basic conformer of the mutant enzyme (see Discussion). At pH 6 and above, the slow phase of the reaction is very similar in both phosphate and nitrate-containing buffers, both with regard to the amplitude of the reaction and to the magnitude and concentration dependence of k_B. To characterize this reaction, we report the average value of k_B, designated k_B^{max}, observed between 2 and 40 μM hydrogen peroxide (Figure 6). We attribute this part of the slow kinetic phase to the isomerization of an unreactive alkaline form of CcP(MI,D235N) to a form which reacts with hydrogen peroxide.

Below pH 6.0, the amplitude of the slow phase of the reaction increases substantially, reaching a maximum amplitude near pH 4.5 (Figure 5). This aspect of the slow kinetic phase is not observed in nitrate-containing buffers. We attribute the slow reaction in this pH region to the conversion of an unreactive acidic form of the mutant enzyme to a form which reacts with hydrogen peroxide. Either the unreactive acidic conformer does not exist in nitrate-containing buffers or it cannot be converted to a reactive form on the time scale of our experiments. Another difference in the slow reaction phase between pH 4 and 5.5 and between pH 6.0 and 8.0 is that the

Table III: Spectroscopic Parameters for Various Heme Proteins and Their Complexes with Ligands

protein	sixth ligand	visible region bands[a] CT1	β	α	CT2	% high-spin
HRP[b-d]	none	496 (10.1)	540 (6.8, sh)	589 (2.4, sh)	642 (2.8)	
Cyt *c'*[e]	none	499 (10.6)	540 (6.7, sh)	593 (1.7, sh)	643 (2.6)	
CcP[f-h]	none	506 (11.4)	544 (8.6, sh)	590 (3.3, sh)	646 (3.4)	100
horse Hb[b,c]	H_2O	499 (9.0)	540 (5.7, sh)	580 (3.2, sh)	632 (4.0)	
human Hb[i-k]	H_2O	500 (9.1)	540 (6.2, sh)	579 (3.7, sh)	630 (4.0)	90
human Hb α[j,k]	H_2O	500 (8.7)	537 (6.4, sh)	576 (3.6, sh)	630 (3.7)	90
human Hb β[j,k]	H_2O	501 (8.6)	531 (8.6)	567 (6.0, sh)	630 (3.4)	65
horse Mb[b,l]	H_2O	505 (9.2)	546 (4.6, sh)	596 (2.2)	630 (3.5)	92
sperm whale Md[m,n]	H_2O	505 (9.5)	543 (5.3, sh)	589 (2.8)	634 (3.6)	89
human Hb[j]	OH^-	488 (8.5, sh)	537 (9.8)	575 (8.8)	600 (6.2, sh)	
human Hb α[j,k]	OH^-		538 (9.9)	575 (8.1)	600 (6.0, sh)	15
human Hb β[j,k]	OH^-		537 (9.4)	570 (7.7)	broad (sh)	5
soybean LegHb[b,i]	OH^-		542 (12.0)	572 (10.6)	602 (sh)	0
sperm whale Mb[d,m,o]	OH^-	485 (8.0, sh)	542 (9.5)	582 (9.1)	595 (8.4)	70
horse Mb[b,l]	OH^-	490 (sh)	543 (8.9)	582 (8.5)	597 (8.6)	
horse Hb[b]	OH^-	481 (sh)	544 (9.7)	576 (8.8)	607 (5.7, sh)	50
HRP[b-d,p]	OH^-		544 (8.6)	577 (6.9)	645 (1.2, sh)	7
soybean LegHb[q]	imidazole	481 (6.7, sh)	526 (10.3)	561 (5.3, sh)		
Cyt b_5[r,s]	imidazole	483 (6.7, sh)	533 (10.2)	561 (8.6, sh)	696 (0.7, sh)	0
Chironomus Hb[t]	imidazole		533 (9.6)	561 (7.6, sh)		
human Hb[j]	imidazole		533 (11.5)	563 (9.0, sh)		
sperm whale Mb[l,n,u]	imidazole		535 (11.1)	568 (7.4, sh)	647 (1.2, sh)	5
heme[v]	imidazole		535	562 (sh)		

[a] Wavelength of absorption maximum given in nanometers. Extinction coefficients are specified in units of mM^{-1} cm^{-1} within the parenthesis; shoulders or inflections in the spectra are identified by an "sh" after the extinction coefficient. [b] George, P., Beetlestone, J., & Griffith, J. S. (1961) in *Haematin Enzymes, Part 1* (Falk, J. E., Lemberg, R., & Morton, R. K., Eds.) pp 105–139, Pergammon Press, Oxford. [c] Keilin, D., & Hartree, E. F. (1951) *Biochem. J. 49*, 88–104. [d] Nozawa, T., Kobayashi, N., & Hatano, M. (1976) *Biochim. Biophys. Acta 427*, 652–662. [e] Taniguchi, S., & Kamen, M. D. (1963) *Biochim. Biophys. Acta 74*, 438–455. [f] Vitello, L. B., Huang, M., & Erman, J. E. (1990) *Biochemistry 29*, 4283–4288. [g] Yonetani, T., & Anni, H. (1987) *J. Biol. Chem. 262*, 9547–9554. [h] Dasgupta, S., Rousseau, D. L., Anni, H., & Yonetani, T. (1989) *J. Biol. Chem. 264*, 654–662. [i] Beetlestone, J. G., & Irvine, D. H. (1968) *J. Chem. Soc. A.* 1340–1346. [j] Yonetani, T., Iizuka, T., & Waterman, M. R. (1971) *J. Biol. Chem. 246*, 7683–7689. [k] Banerjee, R., Alpert, Y., Leterrier, F., & Williams, R. J. P. (1969) *Biochemistry 8*, 2862–2867. [l] Beetlestone, J., & George, P. (1964) *Biochemistry 3*, 707–714. [m] Smith, D. W., & Williams, R. J. P. (1968) *Biochem. J. 110*, 297–301. [n] Diven, W. F., Goldsack, D. E., & Alberty, R. A. (1966) *J. Biol. Chem. 240*, 2437–2441. [o] Hanania, G. I. H., Yegijiayan, A., & Cameron, B. F. (1966) *Biochem. J. 98*, 189–192. [p] Tamura, T. (1971) *Biochim. Biophys. Acta 243*, 249–258. [q] Sievers, G., Gadsby, P. M. A., Peterson, J., & Thomson, A. J. (1983) *Biochim. Biophys. Acta 742*, 637–647. [r] Schnelbacher, E., & Lumper, L. (1971) *Hoppe-Seyler's Z. Physiol. Chem. 352*, 615–628. [s] Bois-Poltoratsky, R., & Ehrenberg, A. (1967) *Eur. J. Biochem. 2*, 361–365. [t] Mohr, P., Scheler, W., Schumann, H., & Müller, K. (1967) *Eur. J. Biochem. 3*, 158–163. [u] Vickery, L., Nozawa, T., & Sauer, K. (1976) *J. Am. Chem. Soc. 98*, 343–349. [v] Peisach, J., & Mims, W. B. (1977) *Biochemistry 16*, 2795–2799.

values of k_B increase with increasing hydrogen peroxide concentration in the more acidic pH region and appear to saturate at high peroxide. Between pH 4.0 and 5.5, the values of k_B as a function of hydrogen peroxide concentration were fit to eq 3. Values of k_B^{max} represent the isomerization rate

$$k_B = k_B^{max}[H_2O_2]/(1 + K[H_2O_2]) \quad (3)$$

from inactive to active acidic conformers in the presence of infinite peroxide. Best-fit values of k_B^{max}, obtained between pH 4 and 5.5, are plotted in Figure 6.

DISCUSSION

pH Dependence of the Electronic Absorption Spectrum and Heme Ligation. Three distinct spectroscopic forms of CcP(MI,D235N) exist between pH 4 and 9 (Figures 1 and 2, Table II). The spectra are typical for high- and low-spin derivatives of Fe(III) heme proteins. The hemes of many common heme proteins are coordinated to the protein through the imidazole group of a histidine residue at one of the heme iron axial sites. The spectroscopic differences between various heme protein derivatives are primarily due to coordination at the second axial position. Coordination of a strong-field ligand, such as cyanide, generates low-spin compounds, while coordination of weak-field ligands, such as fluoride, or pentacoordination generates high-spin species. The energy difference between the low- and high-spin derivatives is small in many heme proteins, and the coordination of ligands such as water, hydroxide, azide, and imidazole gives mixed-spin Fe(III) heme species with high- and low-spin forms in thermal equilibrium (Beetlestone & George, 1964; Smith & Williams, 1968).

Fe(III) heme proteins typically have four absorption bands in the visible region of the spectrum. Two bands, designated the α and β bands, occur near 570 and 540 nm, respectively, and two ligand-to-metal charge-transfer bands occur near 500 and 630 nm (Smith & Williams, 1968; Iizuka & Yonetani, 1970). High-spin derivatives have maxima at the charge-transfer positions with inflections in the absorbance generally observed at the α and β band positions. Low-spin derivatives are dominated by the α and β bands with small or nonexistent charge-transfer bands. On the basis of these spectroscopic criteria, the low-pH form of CcP(MI,D235N) is a high-spin derivative, while the two spectroscopic forms observed between pH 5 and 9 are low-spin species (Figure 1, Table II). This interpretation is consistent with resonance Raman studies (Smulevich et al., 1988) and NMR studies (Satterlee et al., 1990) on the mutant enzyme.

As an aid in identifying the heme ligands in the three forms of CcP(MI,D235N), the spectroscopic properties for a variety of heme protein complexes are collected in Table III. These include pentacoordinate, high-spin species, as well as hexacoordinate aquo, hydroxy, and imidazole forms. The percent high-spin component for the various complexes is also included in Table III when known.

Heme Ligation of CcP(MI,D235N) at pH 6. The X-ray crystallographic structure of CcP(MI,D235N), crystallized

from pH 6 solutions, clearly shows that the mutant enzyme is a hexacoordinate species, with a water (or hydroxide ion) bound to the iron on the distal side of the heme (Wang et al., 1990). Aquo complexes of Fe(III) heme proteins are predominantly high-spin species with maxima at the charge-transfer positions near 500 and 630 nm (Table III). Hydroxy complexes of Fe(III) heme proteins are generally mixed-spin species with the fraction of the high-spin component varying from near 0% to ~70%. The α and β bands are prominent in the hydroxy forms, ranging between 570 and 582 nm for the α band and between 537 and 544 for the β band, Table III. The CcP(MI,D235N) species which predominates in solution at pH 6 is the form designated ls1 in Table II. This species has α and β bands at 576 and 541 nm, respectively (Table II), within the range of values observed for the hydroxy-ligated heme proteins and quite distinct from those for the aquo complexes. Based on the X-ray structure, the absorption spectra, and resonance Raman and NMR studies, the most consistent interpretation of our data is that ls1 is a predominantly low-spin, hydroxy-ligated form of CcP(MI,D235N).

Heme Ligation in the Alkaline Low-Spin Form. All CcP species studied to date, including wild-type yeast CcP, CcP(MI), and all CcP(MI) mutants, exhibit an alkaline, low-spin form with α and β bands near 563 and 532 nm, respectively, with the exception of CcP(MI,H52L) in which a leucine residue replaces the distal histidine (Smulevich et al., 1991). These α and β band positions are essentially identical to the band positions for hemes and heme proteins with imidazole coordinated to both axial positions of the heme iron (Table III). It is reasonable to conclude that the alkaline, low-spin forms of the various CcP's, including the ls2 form of CcP(MI,D235N), have the distal histidine coordinated to the heme iron. This conclusion is supported by the observation that CcP(MI,H52L), the mutant lacking the distal histidine, does not form this low-spin species but rather one that has α and β bands at 580 and 543 nm, the hydroxy-ligated form (Smulevich et al., 1991).

The alkaline, low-spin form of yeast CcP can be induced by heating (Gross & Erman, 1985) or high pH (Dhaliwal & Erman, 1985). The thermally induced form of CcP is associated with a large endothermic transition observed by differential scanning calorimetry (Kresheck & Erman, 1988), suggesting major structural change in the enzyme. We believe that formation of the alkaline, low-spin species in CcP and the mutant enzymes is related to inducing conformational flexibility in the protein at alkaline pH and/or slightly elevated temperature, allowing the distal histidine to coordinate to the heme iron. Coordination of His-52 to the heme iron occurs at significantly lower pH in CcP(MI,D235N) in comparison to CcP(MI) and yeast CcP, suggesting that the *E. coli*-expressed enzymes may be less stable at alkaline pH than wild-type enzyme. The apparent pK_a values for formation of the alkaline form of the enzyme is ~6.5 for CcP(MI,D235N) (Figure 2), 7.8 for CcP(MI), and 8.7 for yeast CcP (Vitello et al., 1990a). The loss of hydrogen peroxide reactivity at alkaline pH correlates very well with formation of the alkaline, bisimidazole, low-spin form for yeast CcP, CcP(MI), and CcP(MI,D235N).

Heme Ligation in the Low-pH, High-Spin Species. Significant differences exist in the spectrum of CcP(MI,D235N) in phosphate and nitrate-containing buffers at pH 4 (Figure 7). The prominent charge-transfer bands near 500 and 630 nm indicate both forms are predominantly high-spin species, but the spectra are so different that a difference in ligation is suggested in the two buffer systems. The high-spin forms are generated by protonation of the hydroxy-ligated species, and conversion to the aquo complex is a reasonable hypothesis. The visible spectrum of the mutant enzyme at pH 4 in nitrate buffer (Figure 7) is nearly identical to that of horse met-myoglobin, an authentic, predominantly high-spin aquo species (Tables II and III). The spectrum of the Asn-235 mutant in nitrate-containing buffers is also similar to those of the Trp-51 mutants in which Ala, Thr, and Met replace Trp-51. These mutants have been shown to be high-spin, hexacoordinate species by EPR spectroscopy (Goodin et al., 1991). The hexacoordinate Trp-51 mutants have long-wavelength charge-transfer bands between 631 and 636 nm compared to 638 nm for CcP(MKI), their parental form, which is ~75% pentacoordinate. The best interpretation of our data is that the high-spin form of CcP(MI,D235N) in nitrate-containing buffer is the hexacoordinated, aquo complex.

At first glance, the spectrum of CcP(MI,D235N) in phosphate buffer at pH 4 (Figure 7) looks very much like the high-spin complexes of CcP formed with anionic ligands such as fluoride, propionate, and acetate (Yonetani & Anni, 1987). The long-wavelength charge-transfer band blue-shifts to 624 nm with an increase in absorptivity while the charge-transfer band at 500 nm has lower absorptivity compared to the spectrum in nitrate-containing buffer (Figure 7, Table II). The absorptivity at the Soret maximum increases with associated loss of absorptivity in the prominent shoulder between 360 and 380 nm. The spectrum of CcP(MI,D235N) in phosphate buffer, pH 4, also resembles that of "aged" CcP, a form of the yeast enzyme which appears after prolonged storage under acidic conditions, especially those containing acetate (Yonetani & Anni, 1987; Smulevich et al., 1989). While it is certain that the aged form of CcP is hexacoordinate, the nature of the ligand has not been identified.

The coordinated ligand of the low-pH form of CcP-(MI,D235N) in phosphate buffer has to be an internal protein residue or a solvent species. The only anionic side chains in the protein at low pH are carboxylate residues. There are no aspartates or glutamates near the heme in CcP(MI,D235N) which could coordinate to the heme iron without major refolding of the protein. The solvent only contains phosphate and water. Phosphate probably does not coordinate to the heme iron. One intriguing possibility is that the heme ligand in pH 4 phosphate buffer remains the hydroxide ion and that the ls1 to hs transition in phosphate buffers is a transition between a predominantly low-spin hydroxy complex to a predominantly high-spin hydroxy complex. The spectrum of CcP(MI,D235N) in pH 4 phosphate buffer is very similar to that predicted for the high-spin form of hydroxy-ligated Fe(III) heme proteins (George et al., 1961). The ls1 to hs transition may be associated with protonation of a group other than the axial hydroxide. This protonation could indirectly weaken the hydroxide–iron bond, either through hydrogen bonding to the ligated hydroxide or changes in protein conformation, triggering the spin-state change. Some support for this possibility exists. The spectrum of CcP(MI,D235N) in deuterium oxide, nitrate or phosphate buffer, pD 6.0, is the same as that observed in aqueous phosphate buffers, pH 4.0 (M. Miller, unpublished observations). Furthermore, the spectrum of the mutant enzyme in deuterium oxide at pD 3.45 is converted to a form with a spectrum of the mutant enzyme in aqueous nitrate buffer, pH 4. This suggests that the enzyme form observed in pH 4, aqueous phosphate buffer can be converted to the spectral form observed in pH 4 aqueous nitrate buffer by protonation of an enzyme group, presumably

the axial hydroxide. If this is true, the heme-bound water has a pK_a less than 4 in phosphate buffer.

The apparent pK_a values for the conversion of the aquo and hydroxy forms of CcP(MI,D235N) are the lowest values for ionization of heme-bound water in any heme protein known to us. Ionization of the heme-bound water in methemoglobins and metmyoglobins is generally between pH 7 and 9 (Antonini & Brunori, 1971) and near pH 11 in horseradish peroxidase.[2] The distal heme pocket in CcP is significantly more polar than that in myoglobin and hemoglobin (Poulos et al., 1980) and can be quite positive, with a formal positive charge on the heme iron and protonation of Arg-48 and His-52. We would expect CcP to bind anionic ligands such as fluoride and cyanide more strongly than metmyoglobin and this is, in fact, observed (Erman, 1974a,b; Antonini & Brunori, 1971). Replacement of Asp-235 with an asparagine residue should increase the net positive charge on the heme iron, increasing its interaction with anions. Preliminary studies indicate that CcP(MI,D235N) binds anions more tightly than yeast CcP [Satterlee et al. (1990); Mauro, unpublished observations]. It may not be unreasonable for the ionization of heme-bound water in CcP(MI,D235N) to have pK_a values below pH 5. The pK_a for the ionization of water bound to the ferric ion in aqueous solution is ~2.2 (George et al., 1961).

A Minimal Mechanism Consistent with the pH-Dependent Properties of CcP(MI,D235N). The pH-dependent spectroscopic and kinetic properties of CcP(MI,D235N) are complex. In this section we develop a minimal mechanism, shown in Figure 8, to rationalize these properties. As with all kinetic mechanisms, we can only claim that this mechanism is consistent with the data and not that it is either unique or correct. However, it is the simplest mechanism that we have found which gives a reasonable fit to all of the data simultaneously. Elimination of any of the species defined in Figure 8 causes significant systematic deviations of the theoretical fit to one or more of the experimental properties measured in this study. The "reasonableness" of the theoretical fits to the data can be judged by inspection of Figures 2 and 4–6.

We began development of the model shown in Figure 8 using the three nondenatured, spectroscopically distinct forms of the enzyme shown in Figure 1 and defined in eq 1. These three enzyme species are not sufficient to explain the pH variation of the stoichiometry and reaction kinetics between the mutant enzyme and hydrogen peroxide. Each of the spectroscopically distinct species must exist in multiple conformational and protonated forms in order to rationalize the hydrogen peroxide reactivity. In Figure 8, the ligation state of the heme iron and the protonation state of the distal histidine residue are explicitly illustrated. Conformational states which affect the reactivity of the enzyme toward peroxide are differentiated schematically by the shape of the line connecting the heme iron and the distal histidine. A minimum of six apparent enzyme ionizations (pK_1–pK_6) are required to explain the reversible pH-dependent behavior of CcP(MI,D235N) between pH 4 and 9. A seventh ionization, pK_7, is required if the denatured enzyme is included (eq 1). Several of the apparent ionizations are similar, and we need to consider microscopic ionization states of the enzyme. For ease in referring to the microscopic states, they are numbered **1**–**10** in Figure 8. The low-pH forms of the enzyme are toward the upper left in the diagram while the high-pH forms are toward the lower right. The high-spin (hs) fors of the enzyme are in the left column, species **1**, **3**, and **5**. The hydroxy-ligated low-spin forms (ls1), species **2**, **4**, **6**, and **8**, are in the center column. The low-spin forms with the distal histidine ligated to the heme iron (ls2) are in the column to the right, species **7**, **9**, and **10**.

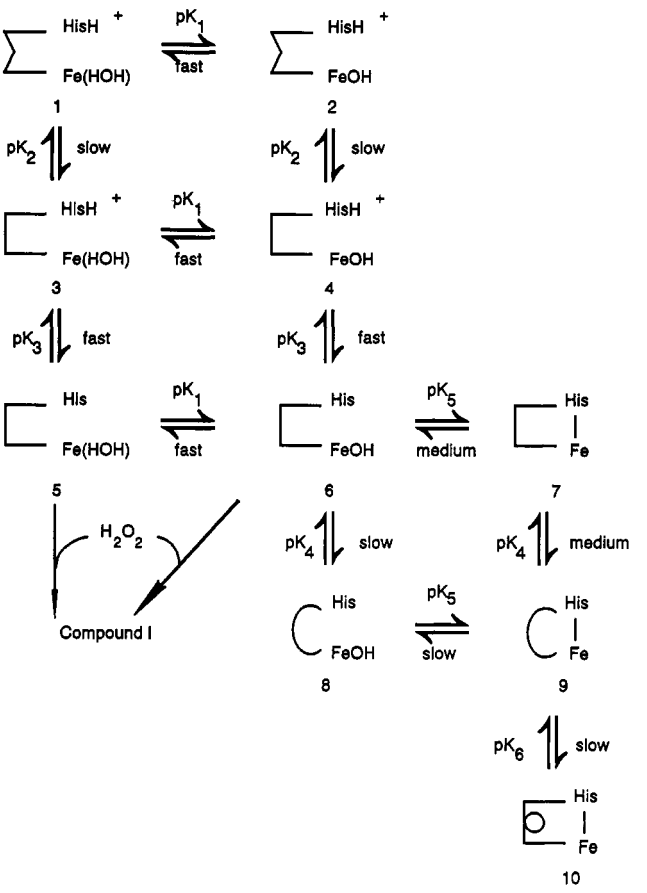

FIGURE 8: Postulated mechanism to rationalize the pH dependence of the spectroscopic properties and hydrogen peroxide reactivity of CcP(MI,D235N). Six pK_a's and 10 microscopic states (indicated by bold numbers) of the enzyme are required. Enzyme denaturation is not shown in this model but occurs at higher pH with an apparent pK_7 of 9.3. The protonation state of the distal histidine and the ligation state of the heme iron are explicitly illustrated in the figure. Different conformation states of the protein are schematically illustrated by the shape of the line connecting the distal histidine and the heme iron. Species **1**, **3**, and **5** are high-spin (hs) forms. The heme-bound water is shown in parenthesis to indicate the uncertainty of the ligation in phosphate buffer. Species **2**, **4**, **6**, and **8** have heme-ligated hydroxide and are responsible for the intermediate-pH, low-spin (ls1) spectrum of the enzyme. Species **7**, **9**, and **10** have the distal histidine coordinated to the heme iron and are responsible for the high-pH, low-spin (ls2) spectrum. The designations "fast", "medium", and "slow" refer to the rate of interconversion between microscopic states relative to the rate of compound I formation. These rates are discussed in the text. In this model, only **5** and **6** react directly with hydrogen peroxide. **3**–**6** equilibrate rapidly compared to compound I formation, and these species are converted to I during the fast bimolecular phase of the hydrogen peroxide reaction. **7** and **9** are converted to I (via **6**) during the slow phase of the hydrogen peroxide reaction. **1**, **2**, **8**, and **10** are not converted to I during the peroxide titration in nitrate-containing buffers.

The interconversion rates between the microscopic states described in Figure 8 are important for interpretation of the experimental observations and these rates are qualitatively described as "fast", "medium", and "slow". These qualitative descriptions are related to the experiments performed in this study which span three different time regimes. Scanning the spectrum of the enzyme, which takes ~8 min, is the longest time-scale experiment performed in this study. Between pH

[2] The acid/alkaline transition in horseradish peroxidase occurs near pH 11 and is associated with the transition from the pentacoordinated acidic form to the hydroxy-ligated alkaline form (Sitter et al., 1988).

4 and ~8, the spectrum of the enzyme is invariant upon rescanning, indicating that the spectral changes induced by pH equilibrate with half-times shorter than ~200 s. Above pH 8, the spectrum does show small changes over extended periods of time but we have not studied these changes in detail and they are not involved in the properties described in this study except to note that enzyme denaturation occurs above pH 9.

The second time regime is characterized by the hydrogen peroxide titration experiments (Figure 4). Adding an aliquot of hydrogen peroxide and measuring the absorbance changes takes ~10 s per titration point. An entire titration of five to six points takes ~1 min. Within the time constraints of the titration, we observe an instantaneous (less than 10 s) increase in absorbance due to compound I formation. The fast absorbance increase is followed by a very slow decrease attributed to compound I decay (Erman & Yonetani, 1976). We have *never* observed a slow *increase* in the amount of I formed during the titration experiments. This means that slow enzyme isomerizations (on the order of tens of seconds or longer), converting unreactive forms into reactive species, do not occur or that compound I decay masks any slow formation of I. Formation of I, either directly or indirectly, occurs with half-times shorter than 10 s.

The third time regime is characterized by the stopped-flow studies, monitoring the fast absorbance changes associated with the hydrogen peroxide reaction. We observe two kinetic phases, a fast bimolecular reaction between hydrogen peroxide and the enzyme and a slower, hydrogen peroxide-independent phase which we attribute to enzyme isomerizations converting unreactive enzyme forms into reactive ones. The pseudo-first-order rate constants for the bimolecular reaction vary between ~0.3 and 230 s^{-1} for the experimental conditions used. The hydrogen peroxide-independent rates, k_B^{max}, vary between 0.15 and 37 s^{-1} (Figure 6).

In Figure 8, the designation "slow" means that the species equilibrate on the time scale of the spectral scanning experiments but cannot be converted to hydrogen peroxide-reactive forms on the time scale of the hydrogen peroxide titration experiments. These slow steps determine the pH dependence of the hydrogen peroxide/enzyme stoichiometry (Figure 4). The interconversions designated "medium" are those which contribute to the slow kinetic phase of the hydrogen peroxide/enzyme reaction. The bimolecular reaction between hydrogen peroxide and the reactive enzyme species is our reference rate, and those steps which equilibrate faster than the hydrogen peroxide reaction (half-times shorter than 3 ms) are designated "fast".

The mechanism shown in Figure 8 is consistent with the experimental data obtained in both nitrate-containing and phosphate buffers. The main differences in the properties of the enzyme between phosphate and nitrate-containing buffers are the apparent pK_a values relating the microscopic states (Table I), the state of ligation in the high-spin form of the mutant enzyme (Figure 7), and the hydrogen peroxide-independent formation of I at acidic pH (Figures 5 and 6). The latter observation is accommodated by making the rate of conversion associated with pK_2 medium in phosphate buffer rather than slow as in nitrate-containing buffer. The mechanism accounts quantitatively for the pH variation of the spectroscopic parameters, the hydrogen peroxide/enzyme reaction stoichiometry, and the pH variation of the apparent bimolecular rate constant and its amplitude and accounts semiquantitatively[3] for the pH variation of the hydrogen peroxide-independent rate constant and its amplitude. All of the lines in the figures correlating properties of CcP(MI,D235N) with pH are calculated using appropriate equations derived from the mechanism. Best-fit values for the pK_a's and their estimated error, obtained by nonlinear least-squares regression analysis of the data obtained in both nitrate-containing the phosphate buffers, are given in Table I.

Bimolecular Reaction between Hydrogen Peroxide and CcP(MI,D235N). Species **3**–**6** are involved in the apparent bimolecular reaction between peroxide and the mutant enzyme. The amplitude of the fast reaction phase is directly proportional to the fraction of enzyme present in these four microscopic states at any pH (Figure 5).

The pH dependence of k_1^{app} (Figure 6) is associated with protonation of the distal histidine, pK_3 in Figure 8. His-52 has been postulated to serve as a base catalyst in the reaction between CcP and hydrogen peroxide (Poulos & Kraut, 1980), and the enzyme is active when His-52 is unprotonated. In Figure 8, **5** and **6** react with hydrogen peroxide to form I. In nitrate buffers, **5** is a minor microscopic form, never exceeding 5% of the enzyme. Protonation of the distal histidine converts **5** and **6** to **3** and **4**. **3** and **4** do not react directly with hydrogen peroxide, but since **3**–**6** equilibrate rapidly compared to the rate of compound I formation, all of these forms are converted to I during the rapid bimolecular phase of the reaction. The apparent bimolecular reaction rate *does* depend upon the relative concentration of these four species, becoming slower as more of the enzyme is in the form of species **3** and **4**. The apparent bimolecular rate constant is given by eq 4. Equation

$$k_1^{app} = k_1([\mathbf{5}] + [\mathbf{6}])/([\mathbf{3}] + [\mathbf{4}] + [\mathbf{5}] + [\mathbf{6}]) \quad (4)$$

4 reduces to eq 2 by expressing the relative concentrations in terms of the total enzyme concentration and K_3. The pH-independent rate constant for the reaction of **5** and **6** (primarily **6**) with hydrogen peroxide is defined as k_1.

The pH-independent bimolecular rate constants for the reaction of **5** and **6** of CcP(MI,D235N) and hydrogen peroxide, k_1, are 11 ± 5 and 9.4 ± 0.8 μM^{-1} s^{-1} in buffers containing nitrate and phosphate, respectively. These values are the same within experimental error and about 4–5 times smaller than the corresponding values for the bimolecular rate constants for yeast CcP and CcP(MI), which are 45 ± 6 and 47 ± 4 μM^{-1} s^{-1}, respectively (Loo & Erman, 1975; Vitello et al., 1990a). Coordination of hydroxide to the heme iron decreases the rate but does not eliminate the reaction. The 4–5-fold decrease in rate between hydrogen peroxide and CcP(MI,D235N) is insignificant in comparison to the reaction rates between hydrogen peroxide and nonenzymatic heme proteins. CcP(MI,D235N) reacts with hydrogen peroxide 4–5 orders of magnitude faster than does aquometmyoglobin or aquomethemoglobin (Dalziel & O'Brien, 1954; George & Irvine, 1956; Yonetani & Schleyer, 1967; Fox et al., 1974), indicating that an open coordination site in the peroxidases is not sufficient to account for the rapid reaction with hydrogen peroxide.

The reaction between hexacoordinate CcP(MI,D235N) and hydrogen peroxide most likely occurs via a dissociative mechanism where the sixth ligand dissociates prior to reaction

[3] The model shown in Figure 8 does not account for the decrease in amplitude of the slow reaction phase between pH 4.5 and 4.0 in phosphate buffer (Figure 5). This observation can be accommodated by including an additional low-pH transition in phosphate buffer or by attributing the observation to the onset of acid denaturation.

with peroxide.[4]

$$\mathrm{CcP(6c)} \underset{k_a}{\overset{k_d}{\rightleftharpoons}} \mathrm{CcP(5c)} \xrightarrow{k[H_2O_2]} \mathrm{CcP{\cdot}I} \qquad (5)$$

Assuming that the pentacoordinate enzyme is in a steady state, the rate of formation of I is given by eq 6. A plot of k_1 as

$$k_1 = k_d k[H_2O_2]/(k_d + k_a + k[H_2O_2]) \qquad (6)$$

a function of hydrogen peroxide concentration should saturate at high peroxide. Although plots of k_A versus hydrogen peroxide are linear within experimental error up to the 40 μM concentrations used in this study, we can estimate lower limits for the parameters defined in eqs 5 and 6. At pH 6, we estimate lower limits for k_d of $\sim$400 s^{-1} and $kk_d/(k_d + k_a)$ of 10 μM^{-1} s^{-1}. The dominant species at pH 6 is **6**, and this analysis suggests that the hydroxide dissociates from the heme at a rate greater than 400 s^{-1}. The apparent bimolecular rate constant of 10 μM^{-1} s^{-1} is a lower limit for the reaction of peroxide with the pentacoordinate form of the enzyme. The true bimolecular rate constant for the pentacoordinate form of the mutant enzyme, k, can be estimated if we can estimate how the enzyme partitions between the penta- and hexacoordinate forms at pH 6. If 33% of the enzyme were pentacoordinate, the true value of k would be greater than 40 μM^{-1} s^{-1}, about the same as observed for yeast CcP and CcP(MI). It is likely that much less than 33% of CcP(MI,D235N) is pentacoordinate,[5] and one could argue that the rate of reaction between hydrogen peroxide and the pentacoordinate form of CcP(MI,D235N) is actually *faster* than the reaction between hydrogen peroxide and pentacoordinate CcP(MI) or wild-type yeast CcP.

The observed bimolecular rate constant depends upon the apparent enzyme ionization characterized by K_3 in Figure 8. The value of pK_3 is 5.4 in nitrate-containing buffers, identical to the pK_a found in CcP(MI) and yeast CcP (Vitello et al., 1990a). This ionization does not seem to influence the absorption spectrum of CcP(MI,D235N) or CcP(MI), although a very careful study shows that this ionization causes a small perturbation in the spectrum of yeast CcP (Conroy & Erman, 1978; Vitello et al., 1990b). This study eliminates the possibility that Asp-235 is the source of the enzyme ionization responsible for the pK_a 5.4 transition. Previous studies have eliminated the heme propionates as the origin of the ionization (Dowe & Erman, 1982). Our current hypothesis is that the pK_3 ionization is associated with His-52.

The value of pK_3 is dependent upon specific ion effects. In CcP(MI,D235N) the values of pK_3 are 5.4 and 4.7 in nitrate-containing and phosphate buffers, respectively. In yeast CcP the corresponding values are 5.4 and about 4 (J. Erman, unpublished observations). The pK_3 values of 4–4.7 in the absence of nitrate seem low for the ionization of a histidine residue but are probably related to the presence of the positively charged Fe(III) heme and Arg-48 in the distal heme pocket. The pK_a for the distal histidine in fluorometmyoglobin is 5.5 (Asher et al., 1981) and this is for a species which has no positive charges in the distal pocket since the fluoride anion neutralizes the net positive charge on the heme iron. We are not aware of any studies determining the pK_a of the distal histidine in aquometmyoglobin, but the pK_a must be less than 5. Krishnamoorthi and La Mar (1984) have found no evidence for the titration of the distal histidine in sperm whale metmyoglobin down to pH 5.0. This work is consistent with that of Carver and Bradbury (1984), who determined the pK_a of the distal histidine in horse and sperm whale carbonmonoxymyoglobins to be 5.0 at 40 °C. The pK_a of the distal histidine in aquometmyoglobin should be lower than that in carbonmonoxymyoglobin due to electrostatic repulsion between the protonated form of His-52 and the positive charge on the heme iron in metmyoglobin. The effect of the positively charged Arg-48 in the distal heme pocket of CcP should lower the pK_a for the distal histidine in CcP to even a greater extent than that in metmyoglobin, and the values of 4–4.7 in the absence of nitrate are reasonable.

When His-52 is protonated, the three positive charges in the distal heme pocket provide a natural anion binding site. Nitrate binding in the distal pocket could stabilize the protonated form of His-52 by effectively neutralizing one of the positive charges. In the nitrate-containing buffer systems we are using, which contain 90–100 mM nitrate, the apparent pK_a for His-52 shifts to 5.4 in the various enzyme species. The shift in the apparent pK_a as a function of nitrate concentration is consistent with previous observations (Loo & Erman, 1975) and with additional studies currently under way in our laboratory (J. Erman, unpublished observations).

Conformational Equilibria Associated with the Heme-Linked Ionizations. In order to explain the pH dependence of the hydrogen peroxide reactions, each of the ligation states of the heme iron must be associated with two or more conformational states of the protein. These conformational states relate hydrogen peroxide-reactive and -unreactive forms of the enzyme. For example, at pH 4 in nitrate buffer, the enzyme is 72% in the hs form and 28% in the ls1 state. Only 20% of the enzyme reacts with hydrogen peroxide (Figure 4A), and most of this reactive enzyme has to be the hs form as determined by the change in absorptivity of the reactive species upon forming I (Figure 4B). This means that, at pH 4, there has to be unreactive hs and ls1 species (**1** and **2**, respectively in Figure 8) as well as reactive (or rapidly converted to reactive) hs and ls1 species (**3** and **4**, respectively in Figure 8). In nitrate buffers, **1** and **2** cannot be converted to reactive forms on the time scale of our titration experiments and formation of **1** and **2** is responsible for the loss of peroxide titer at low pH (Figure 4A). In phosphate buffers, on the other hand, **1** and **2** are converted to **3** and **4** and subsequently to I during the reaction with hydrogen peroxide. This conversion is responsible for the slow phase of the peroxide reaction at low pH (Figures 5 and 6).

At pH 7, the enzyme is 8% in the ls1 form and 92% in the ls2 form. Only 50% of the enzyme reacts with hydrogen peroxide (Figure 4A), and all of this reacts via the slow, hydrogen peroxide-independent phase of the reaction. About half of the ls2 forms are eventually converted to I via the slow reaction phase (**7** and **9**, Figure 8), and half of the ls2 forms cannot be converted to I during the peroxide titration experiments (**10**, Figure 8). **8** is the only ls1 form present at pH 7, and our model fits the data best if **8** cannot be converted to a peroxide reactive form on the time scale of the titration experiments. Conversion of **7** and **9** to **6** and subsequently to I occurs with similar rates in both nitrate and phosphate buffers, with the observed rates varying between 0.15 and 2 s^{-1} (Figure 6).

The peroxide reactivity of the various microscopic species indicate that the transitions involved with pK_2, pK_4, pK_5, and pK_6 are associated with slow (probably conformational)

[4] The reaction between fluoro-CcP and hydrogen peroxide is limited by the rate of fluoride dissociation (J. Erman and C. Britton, unpublished data).

[5] No pentacoordinate forms of CcP(MI,D235N) are observed by resonance Raman spectroscopy between pH 4.5 and 8.5 (Smulevich et al., 1988).

interconversions of the microscopic forms. The transitions involved with pK_1 and pK_3 are fast relative to compound I formation and have half-times smaller than 3 ms. However, in yeast CcP, the ionization associated with the pK_3 5.4 transition is slow on the NMR time scale, again suggesting conformational equilibria are involved (Satterlee & Erman, 1980). Only pK_1, the protonation of the iron-bound hydroxide, may be a true acid dissociation constant in the scheme shown in Figure 8.

We have carried out preliminary pH-jump experiments in which we rapidly change the pH by mixing unbuffered enzyme solutions (usually at pH 4.5 or 7.5) with strongly buffered solutions at the desired final pH in the stopped-flow apparatus. We see up to three kinetic phases with apparent rate constants varying between about 0.8 and 20 s^{-1}, very similar to the hydrogen peroxide-independent rates observed in the reaction between CcP(MI,D235N) and hydrogen peroxide, rates which we have attributed to conformational changes. These rates are too slow to be simple proton association or dissociation reactions. These observations give additional support to the hypothesis that changes in heme ligation are associated with conformational rearrangements in the protein.

The conformation of CcP(MI,D235N) changes as a function of pH, indicating that the conformational changes are triggered by acid/base ionizations in the protein. We can speculate as to the identity of some of these groups and their influence on the structure or reactivity of the mutant enzyme. As discussed above, pK_1 is associated with protonation of the iron-bound hydroxide ion. pK_3 is associated with protonation of His-52, the distal histidine. Its primary effect is on the rate of the reaction with peroxide. Conversion of the ls1 and ls2 forms is associated with coordination of the distal histidine to the heme iron. This coordination also occurs in the ferrous state of the enzyme, where a cooperative, two-proton ionization is involved (Conroy et al., 1978). It has been shown that a CcP mutant in which His-181 has been replaced with a glycine residue also shows this pH-dependent conversion between penta- and hexacoordinate states in the ferrous enzyme but that the conversion occurs via a single proton ionization (Miller et al., 1990), suggesting that ionization of His-181 facilitates coordination of His-52 to the heme iron in the ferrous state. It has been suggested that this is true in the ferric state as well (Smulevich et al., 1991). We speculate that the ionization of His-181 is associated with pK_5 in Figure 8.

Ionizations associated with pK_2, pK_4, and pK_6 are not identified. Possible candidates include the heme propionates and the proximal histidine, His-175, as well as groups remote from the heme.

Conclusions. Replacement of Asp-235 in CcP(MI) with an asparagine residue drastically alters heme ligation in CcP. Between pH 4 and 9, the mutant enzyme can exist in at least four spectroscopically distinct forms depending upon both pH and the nature of the buffer. The most consistent interpretation of the spectroscopic data is that, between pH 7.5 and 9, the enzyme is a hexacoordinate, low-spin form with the distal histidine, His-52, coordinated to the heme iron; between about pH 5 and 6.5, the enzyme is a predominantly low-spin species with hydroxide ion ligated to the heme iron; and at pH 4, in nitrate-containing buffers, the enzyme appears to be a predominantly high-spin aquoheme species. The most unusual spectroscopic state is at pH 4, in phosphate buffers, where the enzyme appears to be a hexacoordinate, high-spin species with an anionic ligand bound to the heme iron. Evidence is presented to suggest that this is a high-spin, hydroxy form of the enzyme.

Each heme ligation state is associated with at least two conformational states of the protein, one which is unreactive toward hydrogen peroxide and one which reacts with hydrogen peroxide or can be converted to a peroxide-reactive form.

Hexacoordination of the heme iron in CcP(MI,D235N) decreases the hydrogen peroxide reaction rate by a factor of 4–5 in comparison to pentacoordinate yeast CcP or CcP(MI). One role of Asp-235 may be to maintain the pentacoordinate state of the native enzyme, but hexacoordination of solvent species (water or hydroxide) in CcP(MI,D235N) has only a minor effect on the peroxide reaction rate in comparison to the very slow peroxide reaction rates observed for nonenzymatic heme proteins such as the globins. Donation of electron density via His-175 and the heme iron to facilitate cleavage of the oxygen–oxygen bond of the peroxide and to stabilize the oxyferryl state does not appear to be a significant role of Asp-235. Assuming a dissociative mechanism for the reaction of hexacoordinate CcP species with hydrogen peroxide, the putative pentacoordinate form of CcP(MI,D235N) reacts more rapidly with peroxide than the pentacoordinate form of either yeast CcP or CcP(MI). The stability of the oxyferryl form of CcP(MI,D235N) is somewhat less than that of yeast CcP (Erman et al., 1992) but significantly more than that of distal-side mutants of CcP (Fishel et al., 1987; Goodin et al., 1991; Erman et al., 1992). The role of Asp-235 may not be involved with activation of hydrogen peroxide but may be involved in maintaining the integrity of the electron-transfer pathway between cytochrome *c* and the oxyferryl group of CcP compound I (Smulevich et al., 1992; Miller & Kraut, 1992).

REFERENCES

Antonini, E., & Brunori, M. (1971) in *Hemoglobin and Myoglobin in Their Reactions with Ligands*, pp 47–48, North-Holland Publishing Co., Amsterdam.

Asher, S. A., Adams, M. L., & Schuster, T. M. (1981) *Biochemistry 20*, 3339–3346.

Balny, C., Anni, H. S., & Yonetani, T. (1987) *FEBS Lett. 221*, 349–354.

Beetlestone, J., & George, P. (1964) *Biochemistry 3*, 707–714.

Carver, J. A., & Bradbury J. H. (1984) *Biochemistry 23*, 4890–4905.

Conroy, C. W., & Erman, J. E. (1978) *Biochim. Biophys. Acta 527*, 370–378.

Conroy, C. W., Tyma, P., Daum, P., & Erman, J. E. (1978) *Biochim. Biophys. Acta 537*, 62–69.

Dalziel, K., & O'Brien, J. R. P. (1954) *Biochem. J. 56*, 648–659.

Dhaliwal, B. K., & Erman, J. E. (1985) *Biochim. Biophys. Acta 827*, 174–182.

Dowe, R. J., & Erman, J. E. (1982) *J. Biol. Chem. 257*, 2403–2405.

Edwards, S. L., Poulos, T. L., & Kraut, J. (1984) *J. Biol. Chem. 259*, 12984–12988.

Erman, J. E. (1974a) *Biochemistry 13*, 34–39.

Erman, J. E. (1974b) *Biochemistry 13*, 39–44.

Erman, J. E., & Yonetani, T. (1976) *Biochim. Biophys. Acta 393*, 350–357.

Erman, J. E., Vitello, L. B., Miller, M. A., & Kraut, J. (1992) *J. Am. Chem. Soc. 114*, 6592–6593.

Fishel, L. A., Villafranca, J. E., Mauro, J. M., & Kraut, J. (1987) *Biochemistry 26*, 351–360.

Fox, J. B., Jr., Nicholas, R. A., Ackerman, S. A., & Swift, C. E. (1974) *Biochemistry 13*, 5178–5186.

George, P., & Irvine, D. H. (1956) *J. Colloid Sci. 11*, 327–336.

George, P., Beetlestone, J., & Griffith, J. S. (1961) in *Haematin Enzymes* (Falk, J. E., Lemberg, R., & Morton, R. K., Eds.) pp 105–139, Pergamon Press, London.

Goodin, D. B., Davidson, M. G., Roe, J. A., Mauk, A. G., & Smith, M. (1991) *Biochemistry 30*, 4953–4962.
Gross, M. T., & Erman, J. E. (1985) *Biochim. Biophys. Acta 830*, 140–146.
Iizuka, T., & Yonetani, T. (1970) *Adv. Biophys. 1*, 157–182.
Kolthoff, I. M., & Belcher, R. (1957) in *Volumetric Analysis*, Vol. III, pp 75–76, Interscience, New York.
Kresheck, G. K., & Erman, J. E. (1988) *Biochemistry 27*, 2490–2496.
Krishnamoorthi, R., & La Mar, G. N. (1984) *Eur. J. Biochem. 138*, 135–140.
Lent, B., Conroy, C. W., & Erman, J. E. (1976) *Arch. Biochem. Biophys. 177*, 56–61.
Loo, S., & Erman, J. E. (1975) *Biochemistry 14*, 3467–3470.
Miller, M. A., & Kraut, J. (1992) *Biophys. J. 61*, A204.
Miller, M. A., Coletta, M., Mauro, J. M., Putnam, L. D., Farnum, M. F., Kraut, J., & Traylor, T. G. (1990) *Biochemistry 29*, 1777–1791.
Poulos, T. L., & Kraut, J. (1980) *J. Biol. Chem. 255*, 8199–8205.
Poulos, T. L., & Finzel, B. C. (1984) *Pept. Protein Rev. 4*, 115–171.
Poulos, T. L., Freer, S. T., Alden, R. A., Edwards, S. L., Skogland, U., Takio, K., Eriksson, B., Xuong, Ng. h., Yonetani, T., & Kraut, J. (1980) *J. Biol. Chem. 255*, 575–580.
Satterlee, J. D., & Erman, J. E. (1980) *Arch. Biochem. Biophys. 202*, 608–616.
Satterlee, J. D., Erman, J. E., Mauro, J. M., & Kraut, J. (1990) *Biochemistry 29*, 8797–8804.
Shelnutt, J. A., Satterlee, J. D., & Erman, J. E. (1983) *J. Biol. Chem. 258*, 2128–2173.
Sitter, A. J., Shifflett, J. R., & Terner, J. (1988) *International Conference on Resonance Spectroscopy* (Clark, R. J. H., & Long, D. A., Eds.) pp 659–660, John Wiley & Sons, Chichester, U.K.
Smith, D. W., & Williams, R. J. P. (1968) *Biochem. J. 110*, 297–301.
Smulevich, G., Mauro, J. M., Fishel, L. A., English, A. M., Kraut, J., & Spiro, T. G. (1988) *Biochemistry 27*, 5477–5485.
Smulevich, G., Mantini, A. R., English, A. M., & Mauro, J. M. (1989) *Biochemistry 28*, 5058–5064.
Smulevich, G., Miller, M. A., Kraut, J., & Spiro, T. (1991) *Biochemistry 30*, 9546–9558.
Vitello, L. B., Erman, J. E., Mauro, J. M., & Kraut, J. (1990a) *Biochim. Biophys. Acta 1038*, 90–97.
Vitello, L. B., Huang, M., & Erman, J. E. (1990b) *Biochemistry 29*, 4283–4288.
Wang, J., Mauro, J. M., Edwards, S. L., Oatley, S. J., Fishel, L. A., Asford, V. A., Xuong, Ng. h., & Kraut, J. (1990) *Biochemistry 29*, 7160–7173.
Yonetani, T., & Schleyer, H. (1967) *J. Biol. Chem. 242*, 1974–1979.
Yonetani, T., & Anni, H. (1987) *J. Biol. Chem. 262*, 9547–9554.

Registry No. Asp, 56-84-8; His, 71-00-1; CcP, 9029-53-2; Asn, 70-47-3; H_2O_2, 7722-84-1; Fe, 7439-89-6; PO_4^{3-}, 14265-44-2; NO_3^-, 14797-55-8.